PLOS GENETICS

RESEARCH ARTICLE

Genome-wide analysis reveals no evidence of trans chromosomal regulation of mammalian immune development

Timothy M. Johanson[1,2☯], Hannah D. Coughlan[1,2☯], Aaron T. L. Lun[1,2], Naiara G. Bediaga[1,2], Gaetano Naselli[1], Alexandra L. Garnham[1,2], Leonard C. Harrison[1,2], Gordon K. Smyth[1,3], Rhys S. Allan[1,2]*

1 The Walter and Eliza Hall Institute of Medical Research, Parkville, Australia, **2** Department of Medical Biology, The University of Melbourne, Parkville, Australia, **3** School of Mathematics and Statistics, The University of Melbourne, Parkville, Australia

☯ These authors contributed equally to this work.
* rallan@wehi.edu.au

Citation: Johanson TM, Coughlan HD, Lun ATL, Bediaga NG, Naselli G, Garnham AL, et al. (2018) Genome-wide analysis reveals no evidence of trans chromosomal regulation of mammalian immune development. PLoS Genet 14(6): e1007431. https://doi.org/10.1371/journal.pgen.1007431

Editor: Gregory S. Barsh, Stanford University School of Medicine, UNITED STATES

Received: December 5, 2017

Accepted: May 18, 2018

Published: June 8, 2018

Data Availability Statement: Human and mouse data are archived on the GEO database under accession numbers GSE105776 and GSE105918 respectively. All other relevant data are within the paper and its Supporting Information files.

Funding: This work was supported by grants and fellowships from the National Health and Medical Research Council of Australia (GKS #1058892, LCH and NGB #1037321, #1129033, #1080887, ATLL and GKS #1054618, RSA and TMJ #1049307, #1100451, TMJ #1124081) and the

Abstract

It has been proposed that interactions between mammalian chromosomes, or transchromosomal interactions (also known as kissing chromosomes), regulate gene expression and cell fate determination. Here we aimed to identify novel transchromosomal interactions in immune cells by high-resolution genome-wide chromosome conformation capture. Although we readily identified stable interactions in *cis*, and also between centromeres and telomeres on different chromosomes, surprisingly we identified no gene regulatory transchromosomal interactions in either mouse or human cells, including previously described interactions. We suggest that advances in the chromosome conformation capture technique and the unbiased nature of this approach allow more reliable capture of interactions between chromosomes than previous methods. Overall our findings suggest that stable transchromosomal interactions that regulate gene expression are not present in mammalian immune cells and that lineage identity is governed by *cis*, not *trans* chromosomal interactions.

Author summary

It is a widely held belief that, in the darkness of the nucleus, strands of DNA that make up different chromosomes frequently meet to 'kiss'. These kisses, or transchromosomal interactions, are thought to be important for the expression of genes and thus cell development. Here, we aimed to identify novel transchromosomal interactions in mouse and human immune cells by high-resolution genome-wide chromosome conformation capture methods. Although we readily identified stable interactions within chromosomes and also between centromeres and telomeres on different chromosomes, surprisingly we identified no gene regulatory transchromosomal interactions in either mouse or human cells, including those previously described. Overall our findings suggest that stable transchromosomal interactions that regulate gene expression are not present in mammalian

Australian Research Council (RSA #130100541). This study was made possible through Victorian State Government Operational Infrastructure Support and Australian Government NHMRC Independent Research Institute Infrastructure Support scheme. The funders had no role in study design, data collection and analysis, decision to publish, or preparation of the manuscript.

Competing interests: The authors have declared that no competing interests exist.

immune cells and that chromosomes are doing far less kissing than was previously believed.

Introduction

Each chromosome contains just one DNA molecule. Recent technological advances have allowed characterisation of the elaborate three-dimensional structures that form from this DNA [1]. These structures include topologically associated domains, which partition the chromosome, and elegant DNA loops that link gene promoters to distant enhancers. In addition to these intrachromosomal structures formed within the same DNA molecule, there are transchromosomal interactions formed between different chromosomes. Relative to intrachromosomal interactions, the frequency, nature and function of transchromosomal interactions are poorly understood [2].

In contrast to the multitude of intrachromosomal interactions known to regulate gene expression, only a handful of transchromosomal interactions have been described. For example, transchromosomal interactions were reported to be crucial for the appropriate expression of a single olfactory gene amongst the ~1300 within the genome [3, 4] and for X chromosome inactivation [5–7]. Interestingly, a large number of the reported transchromosomal interactions have been characterised in cells of the immune system. For example, in both mouse and human T cells the insulin like growth factor 2 (Igf2) locus was reported to interact with a number of loci on different chromosomes [8, 9]. Also in T cells, a regulatory region on mouse chromosome 11 (the T helper 2 locus control region; LCR) was suggested to interact with loci encoding the cytokine interferon gamma (Ifng) on chromosome 10 [10] and interleukin 17 (IL-17) on chromosome 1 [11]. Perturbation of these interactions was associated with altered expression of Ifng and IL-17, respectively. In mouse B cell progenitors, the interaction between the immunoglobulin heavy chain (*Igh*) locus on chromosome 12 and the immunoglobulin light chain (*Igk*) locus on chromosome 6 was important for the rearrangement of the heavy chain locus [12].

These transchromosomal interactions were all identified by either chromatin conformation capture, in which crosslinking, dilution of a ligation reaction and PCR are used to deduce the relative physical proximity of two loci in three-dimensions, or DNA FISH in which microscopy and labelled probes are used to locate loci within individual nuclei, or both. These techniques are targeted approaches. Here we aimed to use an unbiased, genome-wide approach to identify novel gene regulatory transchromosomal interactions in three distinct mouse and human immune cell populations. Unexpectedly, we found very few interactions between chromosomes, and none were gene regulatory or conserved. Overall, our findings question the existence of stable, gene-regulatory transchromosomal interactions underlying immune cell identity.

Results

To elucidate novel transchromosomal interactions, we generated *in situ* HiC libraries from both mouse and human B cells and $CD4^+$ and $CD8^+$ T cells of the immune system (S1A and S1B Fig). The resulting ~200 million paired-end reads were then mapped to the appropriate genome, filtered for artefacts, such as dangling ends and self-circling reads, and counted into 50kb bins with the *diffHic* software package [13]. DNA-DNA interactions were detected by

comparing the interaction intensity in each bin to those surrounding it to determine significant interactions relative to background [14].

Using this pipeline we detected hundreds of interactions between chromosomes in each cell population (S1 Table). Furthermore, our data and publicly available promoter capture HiC data [15] validated numerous previously reported interactions within chromosomes (Fig 1A, S1C–S1E Fig). These include lineage specific interactions [16–18] and others seen in multiple cell lineages [19, 20]. Consistent with previous literature [21], transchromosomal interactions are enriched in gene-rich, centrally located chromosomes (Fig 1B, S2A Fig). However, closer examination of these interactions reveals that a high percentage (74–90% in mouse and 82–94% in human) contain regions recommended to be removed, or 'blacklisted', from analyses due to their high or low mappability, repeated nature, location within telomeres or centromeres, among others [22, 23]. After application of blacklisting the majority of transchromosomal interactions are removed (Fig 1B and 1C, S2 Table). This is in stark contrast to intrachromosomal interactions, of which less than 3% contain blacklisted regions (Fig 1C). The majority of transchromosomal interactions remaining after blacklisting linked regions close to telomeres (Fig 1D and 1E, S2B Fig) or centromeres (Fig 1E, S2C Fig). Thus it appears that the majority of the transchromosomal interactions detected in mammalian immune cells may be a consequence of telomeric and centromeric clustering [24]. Additional experiments would be required to characterize the true specificity and possible functionality of these interactions. Importantly, the detection of these interactions confirms that *in situ* HiC is able to detect interactions between chromosomes.

To determine if any of the detected transchromosomal interactions, whether associated with telomeres or centromeres or not, have a gene regulatory function, we examined the relationship between lineage-specific transchromsomal interactions (those found in only one of the cell populations) (S2 Table) and expression of gene associated with these interactions [25]. In the mouse, we found that the 15 lineage-specific transchromosomal interactions (3 B cell, 8 $CD8^+$ T cell and 4 $CD4^+$ T cell) overlap only 3 genes (*Cct4*, *Lars2*, *Hjurp*) expressed (>5 RPKM) in any of the three lineages and none of these was expressed specifically, or differentially, in the lineage exhibiting the lineage-specific transchromosomal interaction. Similarly, in humans, we found that none of the 38 lineage-specific transchromosomal interactions (18 B cell, 5 $CD8^+$ T cell and 15 $CD4^+$ T cell)(S2 Table) associated with any protein-coding genes differentially expressed (>5 RPKM) in the lineage exhibiting the lineage-specific transchromosomal interaction. This suggests that none of the detected lineage-specific transchromosomal interactions perform a gene regulatory function in mouse or human B or T cells.

It has been suggested that if transchromosomal interactions were functionally important they would be evolutionarily conserved [2]. Therefore, we examined the handful of genes and genomic regions associated with all transchromosomal interactions in mouse and human B and T cells. We found that none of the lineage-specific transchromosomal interactions link orthologous regions in mouse and human.

As we were able to detect transchromosomal interactions, but none of a gene regulatory nature, we examined regions previously reported to be involved in regulatory interactions between chromosomes. We examined our $CD4^+$ T cell data for interactions between the previously mentioned LCR region on mouse chromosome 11 and loci encoding the cytokine interferon gamma (Ifng) on chromosome 10 [10] and interleukin 17 (IL-17) on chromosome 1 [11]. Curiously, no interactions were detected between the LCR and *Ifng* or *IL17* loci in mouse $CD4^+$ T cells (Fig 2A–2D). Intrachromosomal interactions at the loci exhibited three-dimensional structure as expected (Fig 2E and 2F), indicating that the *in situ* HiC data was of sufficient quality. Similarly, in human $CD4^+$ T cells we found no interactions between the LCR and *Ifng* or *IL17* loci (Fig 2G–2J). Again, intrachromosomal interactions at the loci were as expected (Fig 2K and 2L). These analyses were repeated with raw data (no artefact removal

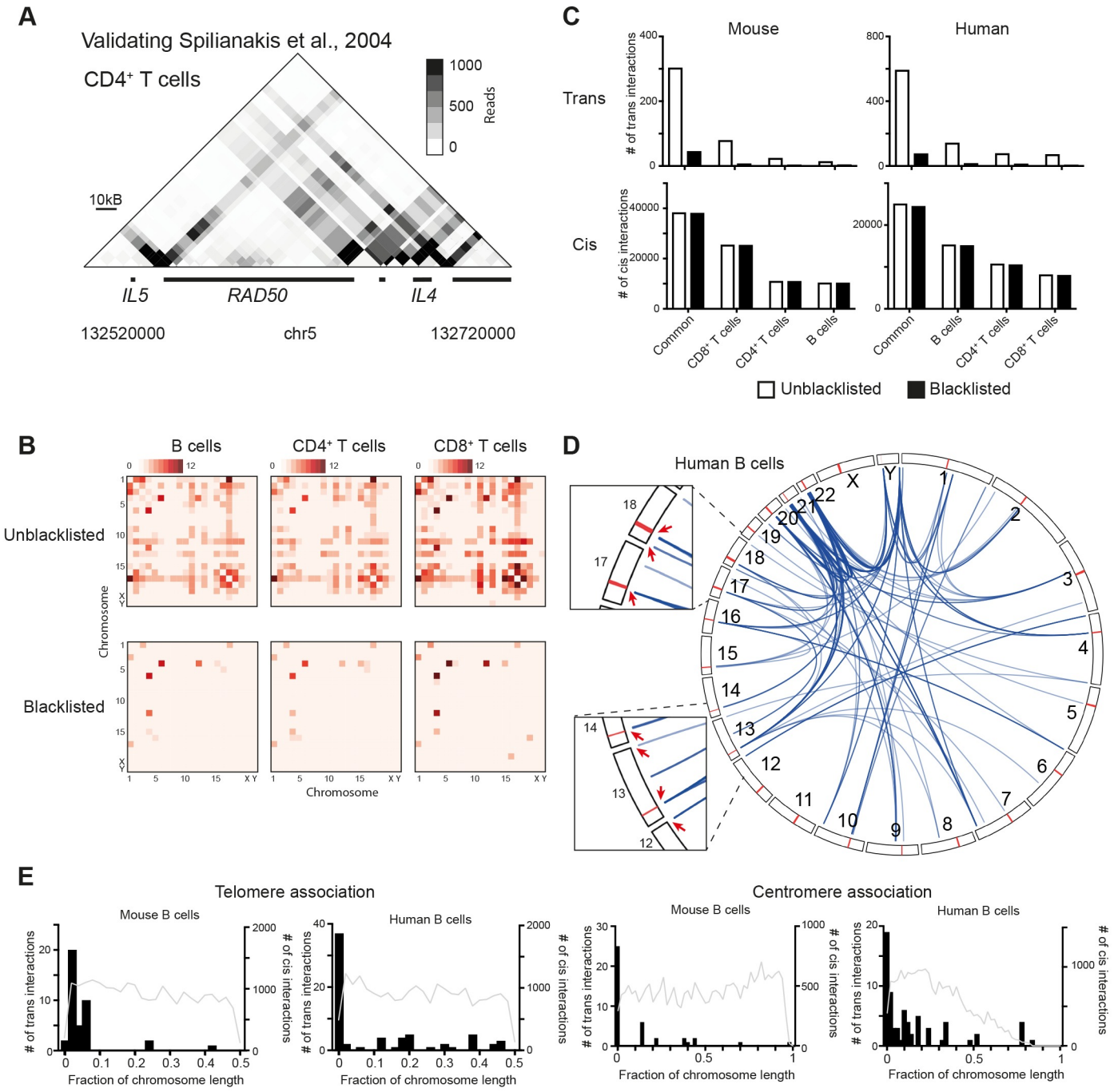

Fig 1. Identification of transchromosomal interactions in mammalian immune cells. (A) Promoter capture HiC contact matrix in human CD4$^+$ T cells confirming intrachromosomal interactions previously reported in the mouse Th2 locus control region **(B)** Heatmaps of chromosomes involved in detected transchromosomal interactions in mouse B cells, CD4$^+$ and CD8$^+$ T cells before and after exclusion of interactions associated with blacklisted regions. **(C)** Numbers of transchromosomal (upper panels) and intrachromosomal interactions (lower panels) common, or unique to murine B cells, CD4$^+$ or CD8$^+$ T cells before (white) and after (black) exclusion of interactions associated with blacklisted regions. **(D)** Circos plot of transchromosomal interactions in human B cells. Insets show examples of interactions associated with centromeres and telomeres. Centromeres are shown in red. **(E)** Association of mouse or human B cell specific transchromosomal (black histogram) and intrachromosomal interactions (grey line) with telomeres or centromeres. The x-axis is normalised to chromosome length starting from the telomere.

https://doi.org/10.1371/journal.pgen.1007431.g001

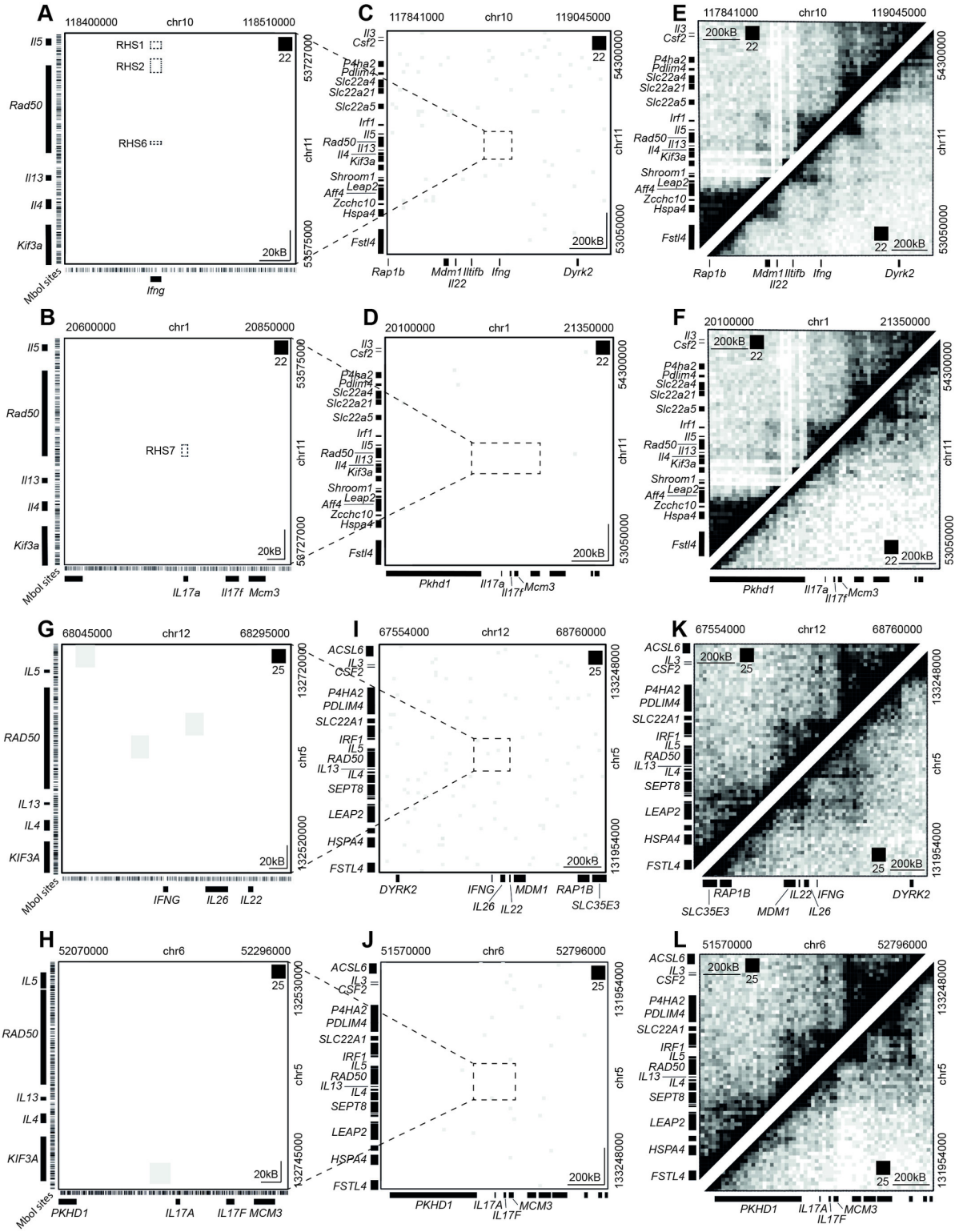

Fig 2. Reported transchromosomal interactions are not detected by *in situ* HiC. (A) HiC contact matrix of regions on chromosome 10 and 11 in mouse CD4$^+$ T cells previously reported to interact. Dotted squares show regions reported to interact. Colour intensity represents interaction with white being absence of detected interaction and black being intense interaction. Pixels are 20kB. **(B)** HiC contact matrix of regions on chromosome 1 and 11 in mouse CD4$^+$ T cells previously reported to interact. Dotted square shows regions reported to interact. **(C)** Expanded HiC contact matrix of regions on chromosome 10 and 11 in mouse CD4$^+$ T cells previously reported to interact. Dotted square

encloses the region shown in Fig 2A. **(D)** Expanded HiC contact matrix of regions on chromosome 1 and 11 in mouse $CD4^+$ T cells previously reported to interact. Dotted square encloses the region shown in Fig 2B. **(E)** HiC contact matrices showing the detected intrachromosomal interactions in mouse $CD4^+$ T cells in the two regions on chromosome 10 and 11 reported to interact in *trans*. **(F)** HiC contact matrices showing the detected intrachromosomal interactions in mouse $CD4^+$ T cells in the two regions on chromosome 1 and 11 reported to interact in *trans*. **(G)** HiC contact matrix of regions on chromosome 12 and 5 in human $CD4^+$ T cells previously reported to interact in mouse $CD4^+$ T cells. **(H)** HiC contact matrix of regions on chromosome 6 and 5 in human $CD4^+$ T cells previously reported to interact in mouse $CD4^+$ T cells. **(I)** Expanded HiC contact matrix of regions on chromosome 12 and 5 in human $CD4^+$ T cells previously reported to interact. Dotted square encloses the region shown in Fig 2G. **(J)** Expanded HiC contact matrix of regions on chromosome 6 and 5 in human $CD4^+$ T cells previously reported to interact in mouse $CD4^+$ T cells. Dotted square encloses the region shown in Fig 2H. **(K)** HiC contact matrices showing the detected intrachromosomal interactions in human $CD4^+$ T cells in the two regions on chromosome 12 and 5 reported to interact in *trans*. **(L)** HiC contact matrices showing the detected intrachromosomal interactions in human $CD4^+$ T cells in the two regions on chromosome 6 and 5 reported to interact in *trans*.

https://doi.org/10.1371/journal.pgen.1007431.g002

step during data processing) to ensure that reads potentially indicating interactions had not been filtered out. No interactions between the LCR and *Ifng* or *IL17* loci in either mouse or human were detected in the raw, unfiltered data (S3A–S3D Fig).

To determine if the depth of sequencing of our *in situ* HiC had inhibited detection of the previously reported transchromosomal interactions, we examined publicly available promoter capture HiC data from human $CD4^+$ T cells [15]. The LCR-*Ifng* or *IL17* interactions were also undetectable in this extremely high-resolution data (S3E and S3F Fig).

We then attempted to detect another previously reported transchromosomal interaction suggested to occur between the immunoglobulin heavy (*Igh*) and light chain (*Igk*) loci in mouse B cell progenitors [12]. Our transchromosomal interaction detection pipeline was applied to *in situ* HiC libraries generated from two B cell progenitors: pro-B cells and immature B cells. Curiously again, using our unbiased, genome-wide approach, we found no interactions between *Igh* on chromosome 12 and *Igk* on chromosome 6 in either B cell progenitor population (S3G and S3H Fig). Intrachromosomal interactions at both loci were as expected (S3G and S3H Fig).

In summary, using an unbiased, genome-wide approach we detect neither novel, nor previously reported, gene-regulatory transchromosomal interactions in three dominant mouse and human immune cell populations.

Discussion

For many years DNA Fluorescent *In situ* Hybridisation (FISH) [26] and chromatin conformation capture (3C) [27] were the dominant technologies used to examine chromosomal interactions, whether in *cis* or *trans*. However, incongruous results from FISH versus 3C within cell types, or in fact from the same technique between studies, has been a persistent issue when examining transchromosomal interactions. For example, two studies reporting transchromosomal interactions between Ifg2 and loci on other chromosomes in mouse T cells found no common interactions [8, 9], while studies of interactions in human T cells found contradictory evidence of interaction [28–30].

To address this vexed issue, we used the *in situ* HiC technique to search for transchromosomal interactions across two species and three distinct cell populations. With this unbiased, genome-wide approach, we were unable to detect any conserved, gene regulatory transchromosomal interactions. While our findings are clear and suggest gene regulatory transchromosomal interactions do not function in the mammalian immune system, it is not possible to be totally conclusive about a negative finding. For example, we cannot rule out gene regulatory interactions that are weak, transient, present in highly repetitive regions or in regions without *Mbo*I restriction sites. Furthermore, because we used only male-derived DNA we could not examine interactions reported to occur between X chromosomes during X chromosome inactivation [31].

Although we were unable to detect gene regulatory transchromosomal interactions, we do detect large numbers of interactions between sub-centromeric and sub-telomeric regions in all cell populations. In addition to demonstrating that *in situ* HiC is able to detect physiologically relevant transchromosomal interactions, these interactions may provide a genomic window into three-dimensional nuclear architecture. For example, changes in interactions in particular centromere associated clusters detected by *in situ* HiC might betray changes in nuclear architecture, such as relocating nucleoli, around which some centromeres are known cluster [32]. These kinds of analyses may also provide insight into previously observed transchromosomal interactions thought to be a consequence of nuclear reorganization [30].

Physiologically relevant transchromosomal interactions that are transient and/or weak may not be detectable by *in situ* HiC. However, this does not explain the absence of the interactions between LCR and *Ifng* or *IL17* loci in T cells, or the immunoglobulin loci in B cell progenitors, as these interactions are reported to occur in 40–50% of cells [10, 12] and the interactions are reported to be as strong as intrachromosomal interactions [10].

Differences between results presented here and those previously reported are likely due to differences in methodology. Previous studies relied on targeted amplification-dependent chromatin capture techniques and/or DNA FISH. It is increasingly clear that even with the appropriate controls [27], a minute amplification bias in a targeting probe combined with the large number of amplification steps required for 3C-based approaches can lead to false positives [2]. Furthermore, it has been suggested that up to half of the ligation events in chromatin capture techniques that rely on dilution of the ligation reaction to deduce proximity, such as 3C or 'dilution' HiC, link regions of DNA that were not truly associated in the intact nucleus [33]. Although DNA-FISH does not exhibit amplification bias, it does suffer from the resolution limitations of light microscopy (250–500nm). Thus it may be that the *Igh* and *Igk* loci in B cell progenitors, or other FISH-demonstrated interactions, frequently lie within hundreds of nanometres of each other, but are nevertheless not sufficiently proximate to be regulatory or chemically crosslinked and thus detected by *in situ* HiC.

In summary, the unbiased, genome-wide *in situ* HiC approach found no evidence for the existence of conserved, lineage-specific, gene regulatory transchromosomal interactions in mammalian immune cells, bringing into question the existence of stable, gene-regulatory transchromosomal interactions underlying immune cell identity.

Materials and methods

Ethics statement

Animal experiments were approved by The Walter and Eliza Hall Institute's animal research ethics committee (No. 2016.003 and 2018.004) and performed under the Australian code for the care and use of animals for scientific purposes. Approval for sourcing of human material and experimentation was obtained from The Walter and Eliza Hall Institute's human research ethics committee (HREC No. 88.03). Results were analysed without blinding of grouping. Anonymized human samples were obtained from a volunteer blood donor registry (http://www.blooddonorregistry.org/home/), which requires donors give consent to their donation being used for research purposes, thus no specific consent was required, or acquired, for the work.

Cell isolation

All animal experiments were performed using C57B/6 male mice at age 6–8 w. Mice were maintained at The Walter and Eliza Hall Institute Animal Facility under specific pathogen–free conditions. Males were randomly chosen from the relevant pool.

Murine $CD4^+$ T cells ($TCR\beta^+$ $CD4^+$ $CD8^-$ $CD44^-$ $CD62L^+$), $CD8^+$ T cells ($TCR\beta^+$ $CD4^-$ $CD8^+$ $CD44^-$ $CD62L^+$), immature B cells ($TCR\beta^-$ $CD19^+$ $B220^+$ IgM^+ IgD^-) and B cells ($TCR\beta^-$ $CD19^+$ $B220^+$ IgM^+ IgD^+) were obtained from mechanically homogenized spleens. Pro-B cells were expanded from B220+ cells from bone marrow on an OP9 cell layer for 7 days in MEM+-Glutamax (Gibco) supplemented with 10mM HEPES, 1mM Sodium Pyruvate, 1x non-essential amino acids (Sigma) and 50μM β-mercaptoethanol (Sigma). At day 7 the IgM- fraction was isolated using immunomagnetic depletion, following manufacturer's instructions.

Cryopreserved human peripheral blood mononuclear cells were thawed and stained with antibodies against human αβ TCR, CD4, CD45RA, CD25, CD14, CD16, HLA-DR, and CD19. $CD4^+$ T cells ($CD14^-$ $CD16^-$ $TCR\alpha\beta^+$ $CD4^+$ $CD45RA^+$ $CD25^-$), $CD8^+$ T cells ($CD14^-$ $CD16^-$ $TCR\alpha\beta^+$ $CD4^-$ $CD45RA^+$ $CD25^-$), and B cells ($TCR\alpha\beta^-$ $HLA\text{-}DR^+$ $CD19^+$) and isolated by flow cytometric sorting.

Flow cytometric analyses were performed on BD FACSCanto with sorting on the BD Aria or Influx (BD Bioscience). Antibodies were purchased from BD Bioscience or eBioscience (S3 Table).

HiC

HiC was performed as previously published [14]. Primary immune cell libraries for both human and mouse were generated in biological duplicate. Libraries were sequenced on an Illumina NextSeq 500 to produce 75bp paired-end reads. Between 160 million and 375 million valid read pairs were generated per sample (S4 Table). Hi-C sequencing data for mouse pro-B cells and immature B cells was obtained from gene expression omnibus accession number GSE99163.

Total RNA isolation

RNA was isolated using the miRNeasy Micro Kit (QIAGEN) following manufacturer's instructions.

RNA-seq analysis

All samples were acquired from two male human donors. Each donor provided one sample per biological condition, giving each condition two replicates. RNA libraries were prepared using an Illumina's TruSeq Total Stranded RNA kit with Ribo-zero Gold (Illumina) according to the manufacturer's instructions. The rRNA-depleted RNA was purified, and reverse transcribed using SuperScript II reverse transcriptase (Invitrogen). Total RNA-Seq libraries were sequenced on the Illumina NextSeq 500 generating 80 base pair paired end reads. The reads were aligned to the human genome (GRCh38/hg38) using the Rsubread aligner [34]. The number of fragments overlapping Ensembl genes were summarized using featureCounts [35].

Differential expression analyses were undertaken using the edgeR [36] and limma [37] software packages. Any gene which did not achieve a count per million mapped reads (CPM) of 0.1 in at least 2 samples was deemed to be unexpressed and subsequently filtered from the analysis. Compositional differences between libraries were normalized using the trimmed mean of log expression ratios (TMM) [38] method. Counts were transformed to $\log_2$-CPM with associated precision weights using voom [39]. Differential expression was assessed using linear models and robust empirical Bayes moderated t-statistics [40]. P-values were adjusted to control the false discovery rate (FDR) below 5% using the Benjamini and Hochberg method. To increase precision, the linear model incorporated a correction for a donor batch effect.

HiC data processing

Read processing and alignment. Reads from each sample were aligned using the presplit_-map.py script in the *diffHic* package v1.4.0 [13]. Briefly, reads were split into 5' and 3' segments if they contained the *Mbo*I ligation signature (GATCGATC), using cutadapt v0.9.5 [41] with default parameters. Segments and unsplit reads were aligned to the GRCm38/mm10 build of the *Mus musculus* genome or the GRCh38/hg38 build of the *Homo sapiens* genome using bowtie2 v2.2.5 [42] in single-end mode. All alignments from a single library were pooled together and the resulting BAM file was sorted by read name. The FixMateInformation command from the Picard suite v1.117 (https://broadinstitute.github.io/picard/) was applied to synchronise mate information for each read pair. Alignments were resorted by position and potential duplicates were marked using the MarkDuplicates command, prior to a final resorting by name. This was repeated for each library generated from each sample in the data set. Each BAM file was further processed to identify the *Mbo*I restriction fragment that each read was aligned to. This was performed using the preparePairs function in *diffHic*, after discarding reads marked as duplicates and those with mapping quality scores below 10. Thresholds were applied to remove artefacts in the libraries, (S4 Table). Read pairs were ignored if one read was unmapped or discarded, or if both reads were assigned to the same fragment in the same orientation. Pairs of inward-facing reads or outward-facing reads on the same chromosome separated by less than a certain distance (min.inward and min.outward respectively) were also treated as dangling ends and were removed. For each read pair, the fragment size was calculated based on the distance of each read to the end of its restriction fragment. Read pairs with fragment sizes above ~1200 bp (max.frag) were considered to be products of off-site digestion and removed. In this manner, approximately 70–75% of read pairs were successfully assigned to restriction fragments in each library. An estimate of alignment error was obtained by comparing the mapping location of the 3' segment of each chimeric read with that of the 5' segment of its mate. If the two segments were not inward-facing and separated by less than ~1200 bp (chim.dist), then a mapping error was considered to be present. Of all the chimeric read pairs for which this evaluation could be performed, around 1–5% were estimated to have errors, indicating that alignment was generally successful. Technical replicates of the same library from multiple sequence runs were then merged with the mergePairs function of *diffHic*.

Data correction and detecting loop interactions. Loop interactions were detected using methods in the *diffHic* package. Read pairs were counted into 50 kbp bin pairs (with bin boundaries rounded up or down to the nearest *MboI* restriction site or blacklisted region edge (see below), respectively) using the *squareCounts* function. Only read pairs mapped to a placed scaffold were included therefore unlocalized and unplaced scaffolds were not included. Mitochondrion read pairs were also excluded.

Looping interactions were detected using a method similar to that described previously [14]. Specifically, read pairs were counted in bin pairs for all libraries of a given cell type or condition. For each bin pair, the log-fold change over the average abundance of each of several neighbouring regions was computed. Neighbouring regions in the interaction space included a square quadrant of sides 'x+1' that was closest to the diagonal and contained the target bin pair in its corner; a horizontal stripe of length '2x+1' centred on the target bin pair; a vertical stripe of '2x+1', similarly centred; and a square of sides '2x+1', also containing the target bin pair in the centre. The enrichment value for each bin pair was defined as the minimum of these log-fold changes, i.e., the bin pair had to have intensities higher than all neighbouring regions to obtain a large enrichment value. These enrichment values were calculated using the *enrichedPairs* function in *diffHic*, with 'x' set to 5 bin sizes (i.e., 250 kbp). Putative loops were

then defined as those with enrichment values above 0.5, with average count across libraries greater than 10, and that were more than 1 bin size away from the diagonal.

Blacklisted regions and removal of centromere and telomere loops. Blacklisted genomic regions were obtained from ENCODE for hg38 and mm10 [23]. Loops that that had at least one anchor in a blacklisted genomic region were removed. Additionally, loops found with an anchor found within a centromere or telomere region as defined by UCSC genome annotation were removed.

Finding overlaps between bin pairs. Overlaps between bin pairs were performed using the overlapsAny function in the InteractionSet package with type = equal and maxgap = 100kb [43]. This considers an overlap to be present if anchors have a separation of less than the maxgap value and if both anchors of the bins pairs overlap.

Promoter capture Hi-C data processing

Promoter capture Hi-C sequencing data for human naive $CD4^+$ T cells was obtained from EGA (https://www.ebi.ac.uk/ega) accession number EGAS00001001911. The read processing and alignment was with the same methods as the Hi-C data except, as the restriction enzyme *Hind*III was used in the assay, the reads were split with a ligation signature of AAGCTAGCTT.

Visualization of results

Plaid plots were constructed using the plotPlaid function from the *diffHic* package. The range of colour intensities in each plot was scaled according to the library size of the sample, to facilitate comparisons between plots from different samples. Heatmaps of the loops between chromosomes where generated using the R package *gplots* with the function *heatmap.2*. Circos plots were generated with the R package RCircos [44].

Supporting information

S1 Fig. Cell sorting strategy and validation of previously reported intrachromosomal interactions. (A) Flow cytometry of homogenised C57BL/6 Pep^{3b} mouse spleen stained with antibodies against TCRβ, CD4, CD8, CD62L, CD44, CD19, B220, IgD and IgM. $CD4^+$ T cells were isolated as $TCR\beta^+$ $CD4^+$ $CD8^-$ $CD62L^+$ $CD44^-$. $CD8^+$ T cells were isolated as $TCR\beta^+$ $CD4^-$ $CD8^+$ $CD62L^+$ $CD44^-$. B cells were isolated as $TCR\beta^-$ $CD19^+$ $B220^+$ IgM^+ IgD^+. **(B)** Flow cytometry of human peripheral blood stained with antibodies against TCRβ, HLA-DR, CD4, CD45RA, CD25, and CD19. $CD4^+$ T cells were isolated as $TCR\beta^+$ $CD4^+$ $CD45RA^-$ $CD25^+$. $CD8^+$ T cells were isolated as $TCR\beta^+$ $CD4^-$ $CD45RA^-$ $CD25^+$. B cells were isolated as $TCR\beta^-$ $HLA\text{-}DR^+$ $CD19^+$. **(C)** HiC contact matrices of mouse immune cells confirming interactions previously reported during mouse neuronal development on mouse chromosome 3 **(D)** HiC contact matrices of mouse immune cells confirming T cell specific interactions previously reported on mouse chromosome 12 **(E)** Promoter capture HiC contact matrices in human $CD4^+$ T cells confirming interactions previously reported in the mouse Hox cluster.
(TIF)

S2 Fig. Examination of transchromosomal interactions in mouse and human immune cells. (A) Heatmap of chromosomes involved in detected transchromosomal interactions in human B cells, $CD4^+$ and $CD8^+$ T cells. **(B)** Association of transchromosomal (black histogram) and intrachromosomal interactions (grey line) in mouse or human $CD8^+$ or $CD4^+$ T cells with telomeres. The x-axis is normalised to chromosome length starting from the telomere. **(C)** Association of transchromosomal (black histogram) and intrachromosomal interactions (grey line) in mouse or human $CD8^+$ or $CD4^+$ T cells with centromeres. The x-axis is

normalised to chromosome length starting from the centromere.
(TIF)

S3 Fig. Reported transchromosomal interactions are not detected by *in situ* HiC, unfiltered *in situ* HiC or promoter capture HiC. (A) HiC contact matrix of unfiltered data of regions on chromosome 10 and 11 in mouse $CD4^+$ T cells previously reported to interact. Colour intensity represents interaction with white being absence of detected interaction and black being intense interaction. Pixels are 20kB. **(B)** HiC contact matrix of unfiltered data of regions on chromosome 12 and 5 in human $CD4^+$ T cells previously reported to interact. **(C)** HiC contact matrix of unfiltered data of regions on chromosome 1 and 11 in mouse $CD4^+$ T cells previously reported to interact. **(D)** HiC contact matrix of unfiltered data of regions on chromosome 6 and 5 in human $CD4^+$ T cells previously reported to interact. **(E)** Promoter capture HiC contact matrix [15] of regions on chromosome 12 and 5 in human $CD4^+$ T cells previously reported to interact. **(F)** Promoter capture HiC contact matrix [15] of regions on chromosome 6 and 5 in human $CD4^+$ T cells previously reported to interact. **(G)** HiC contact matrices of regions on chromosome 12 and 6 in mouse pro-B cells previously reported to interact in these cells. The left panel is an expanded plot of the region enclosed by the dotted square in the central panel. The right panel shows the intrachromosomal interactions in the same regions. **(H)** HiC contact matrices of regions on chromosome 12 and 6 in mouse immature B cells previously reported to interact in these cells. The left panel is an expanded plot of the region enclosed by the dotted square in the central panel. The right panel shows the intrachromosomal interactions in the same regions.
(TIF)

S1 Table. Detected transchromosomal interactions.
(PDF)

S2 Table. Post-blacklisting transchromosomal interactions.
(PDF)

S3 Table. Antibodies used in study.
(PDF)

S4 Table. Details of in situ HiC libraries.
(PDF)

Author Contributions

Conceptualization: Timothy M. Johanson, Hannah D. Coughlan, Aaron T. L. Lun, Naiara G. Bediaga, Gaetano Naselli, Alexandra L. Garnham, Leonard C. Harrison, Gordon K. Smyth, Rhys S. Allan.

Data curation: Hannah D. Coughlan, Naiara G. Bediaga, Alexandra L. Garnham, Gordon K. Smyth.

Formal analysis: Timothy M. Johanson, Hannah D. Coughlan, Naiara G. Bediaga, Gaetano Naselli, Alexandra L. Garnham.

Funding acquisition: Leonard C. Harrison, Gordon K. Smyth, Rhys S. Allan.

Investigation: Timothy M. Johanson, Hannah D. Coughlan, Naiara G. Bediaga, Gaetano Naselli.

Methodology: Hannah D. Coughlan, Aaron T. L. Lun, Gaetano Naselli, Alexandra L. Garnham.

Project administration: Leonard C. Harrison, Gordon K. Smyth, Rhys S. Allan.

Resources: Gaetano Naselli, Leonard C. Harrison.

Software: Hannah D. Coughlan, Aaron T. L. Lun.

Supervision: Leonard C. Harrison, Gordon K. Smyth, Rhys S. Allan.

Visualization: Timothy M. Johanson, Hannah D. Coughlan, Aaron T. L. Lun.

Writing – original draft: Timothy M. Johanson, Hannah D. Coughlan, Rhys S. Allan.

Writing – review & editing: Timothy M. Johanson, Hannah D. Coughlan, Aaron T. L. Lun, Naiara G. Bediaga, Gaetano Naselli, Leonard C. Harrison, Gordon K. Smyth, Rhys S. Allan.

References

1. Yu M, Ren B. The Three-Dimensional Organization of Mammalian Genomes. Annu Rev Cell Dev Biol. 2017. Epub 2017/08/09. https://doi.org/10.1146/annurev-cellbio-100616-060531 PMID: 28783961.
2. Williams A, Spilianakis CG, Flavell RA. Interchromosomal association and gene regulation in trans. Trends Genet. 2010; 26(4):188–97. Epub 2010/03/20. https://doi.org/10.1016/j.tig.2010.01.007 PMID: 20236724; PubMed Central PMCID: PMCPMC2865229.
3. Clowney EJ, LeGros MA, Mosley CP, Clowney FG, Markenskoff-Papadimitriou EC, Myllys M, et al. Nuclear aggregation of olfactory receptor genes governs their monogenic expression. Cell. 2012; 151 (4):724–37. Epub 2012/11/13. https://doi.org/10.1016/j.cell.2012.09.043 PMID: 23141535; PubMed Central PMCID: PMCPMC3659163.
4. Lomvardas S, Barnea G, Pisapia DJ, Mendelsohn M, Kirkland J, Axel R. Interchromosomal interactions and olfactory receptor choice. Cell. 2006; 126(2):403–13. Epub 2006/07/29. https://doi.org/10.1016/j.cell.2006.06.035 PMID: 16873069.
5. Bacher CP, Guggiari M, Brors B, Augui S, Clerc P, Avner P, et al. Transient colocalization of X-inactivation centres accompanies the initiation of X inactivation. Nat Cell Biol. 2006; 8(3):293–9. Epub 2006/01/26. https://doi.org/10.1038/ncb1365 PMID: 16434960.
6. Xu N, Tsai CL, Lee JT. Transient homologous chromosome pairing marks the onset of X inactivation. Science. 2006; 311(5764):1149–52. Epub 2006/01/21. https://doi.org/10.1126/science.1122984 PMID: 16424298.
7. Zhang LF, Huynh KD, Lee JT. Perinucleolar targeting of the inactive X during S phase: evidence for a role in the maintenance of silencing. Cell. 2007; 129(4):693–706. Epub 2007/05/22. https://doi.org/10.1016/j.cell.2007.03.036 PMID: 17512404.
8. Ling JQ, Li T, Hu JF, Vu TH, Chen HL, Qiu XW, et al. CTCF mediates interchromosomal colocalization between Igf2/H19 and Wsb1/Nf1. Science. 2006; 312(5771):269–72. Epub 2006/04/15. https://doi.org/10.1126/science.1123191 PMID: 16614224.
9. Zhao Z, Tavoosidana G, Sjolinder M, Gondor A, Mariano P, Wang S, et al. Circular chromosome conformation capture (4C) uncovers extensive networks of epigenetically regulated intra- and interchromosomal interactions. Nat Genet. 2006; 38(11):1341–7. Epub 2006/10/13. https://doi.org/10.1038/ng1891 PMID: 17033624.
10. Spilianakis CG, Lalioti MD, Town T, Lee GR, Flavell RA. Interchromosomal associations between alternatively expressed loci. Nature. 2005; 435(7042):637–45. Epub 2005/05/10. https://doi.org/10.1038/nature03574 PMID: 15880101.
11. Kim LK, Esplugues E, Zorca CE, Parisi F, Kluger Y, Kim TH, et al. Oct-1 regulates IL-17 expression by directing interchromosomal associations in conjunction with CTCF in T cells. Mol Cell. 2014; 54(1):56–66. Epub 2014/03/13. https://doi.org/10.1016/j.molcel.2014.02.004 PMID: 24613343; PubMed Central PMCID: PMCPMC4058095.
12. Hewitt SL, Farmer D, Marszalek K, Cadera E, Liang HE, Xu Y, et al. Association between the Igk and Igh immunoglobulin loci mediated by the 3' Igk enhancer induces 'decontraction' of the Igh locus in pre-B cells. Nat Immunol. 2008; 9(4):396–404. Epub 2008/02/26. https://doi.org/10.1038/ni1567 PMID: 18297074; PubMed Central PMCID: PMCPMC2583163.
13. Lun AT, Smyth GK. diffHic: a Bioconductor package to detect differential genomic interactions in Hi-C data. BMC Bioinformatics. 2015; 16:258. https://doi.org/10.1186/s12859-015-0683-0 PMID: 26283514; PubMed Central PMCID: PMCPMC4539688.

14. Rao SS, Huntley MH, Durand NC, Stamenova EK, Bochkov ID, Robinson JT, et al. A 3D map of the human genome at kilobase resolution reveals principles of chromatin looping. Cell. 2014; 159(7):1665–80. https://doi.org/10.1016/j.cell.2014.11.021 PMID: 25497547.

15. Javierre BM, Burren OS, Wilder SP, Kreuzhuber R, Hill SM, Sewitz S, et al. Lineage-Specific Genome Architecture Links Enhancers and Non-coding Disease Variants to Target Gene Promoters. Cell. 2016; 167(5):1369–84 e19. https://doi.org/10.1016/j.cell.2016.09.037 PMID: 27863249; PubMed Central PMCID: PMCPMC5123897.

16. Isoda T, Moore AJ, He Z, Chandra V, Aida M, Denholtz M, et al. Non-coding Transcription Instructs Chromatin Folding and Compartmentalization to Dictate Enhancer-Promoter Communication and T Cell Fate. Cell. 2017; 171(1):103–19 e18. Epub 2017/09/25. https://doi.org/10.1016/j.cell.2017.09.001 PMID: 28938112; PubMed Central PMCID: PMCPMC5621651.

17. Li L, Zhang JA, Dose M, Kueh HY, Mosadeghi R, Gounari F, et al. A far downstream enhancer for murine Bcl11b controls its T-cell specific expression. Blood. 2013; 122(6):902–11. https://doi.org/10.1182/blood-2012-08-447839 PMID: 23741008; PubMed Central PMCID: PMCPMC3739036.

18. Spilianakis CG, Flavell RA. Long-range intrachromosomal interactions in the T helper type 2 cytokine locus. Nat Immunol. 2004; 5(10):1017–27. Epub 2004/09/21. https://doi.org/10.1038/ni1115 PMID: 15378057.

19. Schoenfelder S, Sugar R, Dimond A, Javierre BM, Armstrong H, Mifsud B, et al. Polycomb repressive complex PRC1 spatially constrains the mouse embryonic stem cell genome. Nat Genet. 2015; 47 (10):1179–86. Epub 2015/09/01. https://doi.org/10.1038/ng.3393 PMID: 26323060; PubMed Central PMCID: PMCPMC4847639.

20. Bonev B, Mendelson Cohen N, Szabo Q, Fritsch L, Papadopoulos GL, Lubling Y, et al. Multiscale 3D Genome Rewiring during Mouse Neural Development. Cell. 2017; 171(3):557–72 e24. Epub 2017/10/21. https://doi.org/10.1016/j.cell.2017.09.043 PMID: 29053968; PubMed Central PMCID: PMCPMC5651218.

21. Lieberman-Aiden E, van Berkum NL, Williams L, Imakaev M, Ragoczy T, Telling A, et al. Comprehensive mapping of long-range interactions reveals folding principles of the human genome. Science. 2009; 326(5950):289–93. Epub 2009/10/10. https://doi.org/10.1126/science.1181369 PMID: 19815776; PubMed Central PMCID: PMCPMC2858594.

22. Chakraborty A, Ay F. Identification of copy number variations and translocations in cancer cells from Hi-C data. bioRxiv. 2017. https://doi.org/10.1101/179275

23. Consortium EP. An integrated encyclopedia of DNA elements in the human genome. Nature. 2012; 489 (7414):57–74. Epub 2012/09/08. https://doi.org/10.1038/nature11247 PMID: 22955616; PubMed Central PMCID: PMCPMC3439153.

24. Weierich C, Brero A, Stein S, von Hase J, Cremer C, Cremer T, et al. Three-dimensional arrangements of centromeres and telomeres in nuclei of human and murine lymphocytes. Chromosome Res. 2003; 11(5):485–502. Epub 2003/09/16. PMID: 12971724.

25. Heng TS, Painter MW, Immunological Genome Project C. The Immunological Genome Project: networks of gene expression in immune cells. Nat Immunol. 2008; 9(10):1091–4. https://doi.org/10.1038/ni1008-1091 PMID: 18800157.

26. Rudkin GT, Stollar BD. High resolution detection of DNA-RNA hybrids in situ by indirect immunofluorescence. Nature. 1977; 265(5593):472–3. Epub 1977/02/03. PMID: 401954.

27. Dekker J, Rippe K, Dekker M, Kleckner N. Capturing chromosome conformation. Science. 2002; 295 (5558):1306–11. Epub 2002/02/16. https://doi.org/10.1126/science.1067799 PMID: 11847345.

28. LaSalle JM, Lalande M. Homologous association of oppositely imprinted chromosomal domains. Science. 1996; 272(5262):725–8. Epub 1996/05/03. PMID: 8614834.

29. Nogami M, Kohda A, Taguchi H, Nakao M, Ikemura T, Okumura K. Relative locations of the centromere and imprinted SNRPN gene within chromosome 15 territories during the cell cycle in HL60 cells. J Cell Sci. 2000; 113 (Pt 12):2157–65. Epub 2000/05/29. PMID: 10825289.

30. Teller K, Solovei I, Buiting K, Horsthemke B, Cremer T. Maintenance of imprinting and nuclear architecture in cycling cells. Proc Natl Acad Sci U S A. 2007; 104(38):14970–5. Epub 2007/09/13. https://doi.org/10.1073/pnas.0704285104 PMID: 17848516; PubMed Central PMCID: PMCPMC1986597.

31. Augui S, Nora EP, Heard E. Regulation of X-chromosome inactivation by the X-inactivation centre. Nat Rev Genet. 2011; 12(6):429–42. Epub 2011/05/19. https://doi.org/10.1038/nrg2987 PMID: 21587299.

32. Prieto JL, McStay B. Nucleolar biogenesis: the first small steps. Biochem Soc Trans. 2005;33(Pt 6):1441–3. Epub 2005/10/26.

33. Nagano T, Varnai C, Schoenfelder S, Javierre BM, Wingett SW, Fraser P. Comparison of Hi-C results using in-solution versus in-nucleus ligation. Genome Biol. 2015; 16:175. Epub 2015/08/27. https://doi.org/10.1186/s13059-015-0753-7 PMID: 26306623; PubMed Central PMCID: PMCPMC4580221.

34. Liao Y, Smyth GK, Shi W. The Subread aligner: fast, accurate and scalable read mapping by seed-and-vote. Nucleic Acids Res. 2013; 41(10):e108. https://doi.org/10.1093/nar/gkt214 PMID: 23558742; PubMed Central PMCID: PMCPMC3664803.

35. Liao Y, Smyth GK, Shi W. featureCounts: an efficient general purpose program for assigning sequence reads to genomic features. Bioinformatics. 2014; 30(7):923–30. https://doi.org/10.1093/bioinformatics/btt656 PMID: 24227677.

36. McCarthy DJ, Chen Y, Smyth GK. Differential expression analysis of multifactor RNA-Seq experiments with respect to biological variation. Nucleic Acids Res. 2012; 40(10):4288–97. https://doi.org/10.1093/nar/gks042 PMID: 22287627; PubMed Central PMCID: PMCPMC3378882.

37. Ritchie ME, Phipson B, Wu D, Hu Y, Law CW, Shi W, et al. limma powers differential expression analyses for RNA-sequencing and microarray studies. Nucleic Acids Res. 2015; 43(7):e47. https://doi.org/10.1093/nar/gkv007 PMID: 25605792; PubMed Central PMCID: PMCPMC4402510.

38. Robinson MD, Oshlack A. A scaling normalization method for differential expression analysis of RNA-seq data. Genome Biol. 2010; 11(3):R25. https://doi.org/10.1186/gb-2010-11-3-r25 PMID: 20196867; PubMed Central PMCID: PMCPMC2864565.

39. Law CW, Chen Y, Shi W, Smyth GK. voom: Precision weights unlock linear model analysis tools for RNA-seq read counts. Genome Biol. 2014; 15(2):R29. Epub 2014/02/04. https://doi.org/10.1186/gb-2014-15-2-r29 PMID: 24485249; PubMed Central PMCID: PMCPMC4053721.

40. Phipson B, Lee S, Majewski IJ, Alexander WS, Smyth GK. Robust hyperparameter estimation protects against hypervariable genes and improves power to detect differential expression. Annals of Applied Statistics. 2016; 10.

41. Martin M. Cutadapt removes adapter sequences from high-throughput sequencing reads. EMBnet journal. 2011; 17(1):pp. 10–2.

42. Langmead B, Salzberg SL. Fast gapped-read alignment with Bowtie 2. Nat Methods. 2012; 9(4):357–9. https://doi.org/10.1038/nmeth.1923 PMID: 22388286; PubMed Central PMCID: PMCPMC3322381.

43. Lun AT, Smyth GK. csaw: a Bioconductor package for differential binding analysis of ChIP-seq data using sliding windows. Nucleic Acids Res. 2016; 44(5):e45. https://doi.org/10.1093/nar/gkv1191 PMID: 26578583; PubMed Central PMCID: PMCPMC4797262.

44. Zhang H, Meltzer P, Davis S. RCircos: an R package for Circos 2D track plots. BMC Bioinformatics. 2013; 14:244. Epub 2013/08/14. https://doi.org/10.1186/1471-2105-14-244 PMID: 23937229; PubMed Central PMCID: PMCPMC3765848.